REVISTA MATÉRIA V.28 N.4
ISSN 1517-7076 articles e20230186, 2023

Structural performance of hybrid FRP laminates on concrete beams made with manufactured sand

Manikandan Kesavakannan[1], Ramasamy Vasudevan[2]

[1]Dhanalakshmi Srinivasan Engineering College (Autonomous), Department of Civil Engineering. Perambalur, Tamil Nadu, India.

[2]Adhiparasakthi Engineering College, Department of Civil Engineering. Melmaruvathur, Chengalpattu, Tamil Nadu, India.

e-mail: rkmanish@outlook.com, rams_apec@yahoo.co.in

ABSTRACT

Concrete, a vital material in construction, is facing challenges in enhancing its strength and durability. Researchers are exploring innovative approaches, such as using Fibre Reinforced Polymer (FRP) composites, to improve these properties. Structural flaws are often found during evaluations of existing buildings, especially older ones that may benefit from retrofitting. In this study, Manufactured sand was tested as a replacement for fine aggregate in concrete mixes to strengthen the mixes. The study utilized response surface methodology to predict the strength properties of sustainable Concrete mixes based on compressive strength. The flexure of reinforced concrete beams was evaluated using chopped strand mat (CSM) and glass-fiber reinforced plastic (GFRP) laminates. The study tested five RC beams using a 4-point bending configuration, with one beam serving as the control and the other four strengthened with FRP laminates. The results showed successful improvement in load-bearing capacity with GFRP + CSM laminates. However, thicker FRP sheets were not recommended as they can impact flexural strength. The GFRP + CSM enhanced beam achieved a 107% increase in ultimate load compared to the non-strengthened beams, according to experimental results. The strengthened beam had a greater rise load-carrying capability of 115 kN than the unstrengthen beam.

Keywords: Response surface methodology; Manufactured sand; composite materials; flexure; RC beams; strengthening.

1. INTRODUCTION

Concrete plays a major role in deciding the strength and durability of structures with reference to certain limitations. Due to its better performance and flexibility in handling the major structures are built using concrete and moreover carry a good amount of compression [1]. In order to create concrete, you need to combine cement, water, and different aggregates, such sand, gravel, or crushed stone. It is a widely utilised and adaptable material in construction for a variety of uses, such as foundations, walls, floors, highways, bridges, and dams. Cement, water, and aggregates are commonly combined to create a thick paste while making concrete. After that, the paste is poured into a mould or shape and let to cure and harden. The concrete must cure in order to reach its maximum strength and durability, therefore curing is crucial. There are numerous varieties of concrete, each with special qualities and applications [2, 3]. For instance, certain varieties of concrete are made to endure high pressures or extremely high temperatures, while others are made purely for aesthetic reasons. Concrete offers a number of advantages, but it also has some disadvantages. For instance, if it is not properly maintained, it may crack or degrade over time and be heavy and challenging to work with. Concrete may, nevertheless, be a very strong and long-lasting building material when used with suitable design and construction methods. Steel reinforcement bars are included in RCC to boost its strength and durability. The concrete is given more support and strength by the steel reinforcement, which increases its resistance to bending and tensile stresses. Construction of buildings, bridges, dams, and other structures requiring strength and longevity frequently makes use of RCC [4–6]. The formwork or mould must be ready, the steel reinforcement must be contained within it, and then the concrete must be poured into the mould to complete the RCC construction process. The formwork is removed after the concrete has dried and hardened, and the reinforced concrete structure is then ready for use. The strength and durability of RCC are two of its key benefits. By incorporating reinforcement, concrete may handle greater loads and hold up against cracking and deformation better than unreinforced concrete. Moreover, RCC

Corresponding Author: Manikandan Kesavakannan Received on 27/06/2023 Accepted on 15/08/2023

DOI: https://doi.org/10.1590/1517-7076-RMAT-2023-0186

is resistant to fire and has effective sound-insulating qualities. However, be more expensive and time-consuming to build than plain concrete since it needs extra work and materials for the placement and fastening of the reinforcement. RCC is still a preferred option for numerous construction projects [7, 8].

Response Surface Methodology (RSM) is a statistical technique used to explore the relationship between input variables and a response of interest. It is particularly useful for studying the impact of multiple factors and their interactions. RSM aims to determine optimal values for the input variables that yield the desired response. By systematically varying the variables and observing the corresponding responses, RSM identifies critical factors and their optimal settings. This method involves design of experiments, regression analysis, and graphical visualization to fit mathematical models to the experimental data [9]. Central Composite Design (CCD) is a popular approach within RSM, combining factorial design with additional points to estimate curvature. CCD allows for a comprehensive understanding of linear, quadratic, and interaction effects. It involves factorial, axial, and center points to estimate main effects, curvature, and experimental error. CCD facilitates the estimation of response surface models, enabling prediction, optimization, and analysis of the system. RSM and CCD find applications in various fields such as engineering, manufacturing, pharmaceuticals, and agriculture. A polymer matrix that has been strengthened with fibres is the basis of a composite material known as FRP. Carbon or glass are just a few of the materials that can be used to create fibers. Epoxy/polyester/vinyl ester resin are frequently used to create polymer matrixes [10]. The excellent strength-to-weight ratio, corrosion resistance, and longevity of FRP composites are well known. They are frequently utilised in a variety of industries, including the sporting goods, aerospace, automotive, construction, and maritime sectors. FRP composites are frequently used in construction to reinforce and strengthen concrete structures like bridges, columns, and beams. They can also be applied to the renovation and upkeep of existing buildings. FRP composites are highly adaptable and effective materials that have several benefits over conventional materials. FRP is a composite material comprising strong fibers embedded in a polymer matrix. When used as reinforcement in concrete structures, FRP offers several advantages to enhance concrete strength and performance. FRP has a high strength-to-weight ratio, reducing the overall weight of the structure while maintaining its strength and stiffness. It is corrosion-resistant, eliminating the risk of corrosion-related degradation. By providing high tensile strength, FRP reinforcement significantly improves the concrete element's overall tensile strength and flexural capacity. FRP materials can be tailored for specific flexural behavior, optimizing the structure's response to applied loads. Additionally, FRP provides increased ductility, aiding energy dissipation during extreme events. Its ease of installation, non-magnetic and non-conductive properties, aesthetics, and design flexibility further contribute to its widespread use as an effective concrete reinforcement material. Proper design, detailing, and installation are essential to fully harness the benefits of FRP in composite sections.

A thermosetting resin is used to create the composite material known as GFRP. Glass fibres contribute to the material's high strength and stiffness, and resin binds the fibres together and protects them from damage. Because to its excellent strength-to-weight ratio, resistance to corrosion, and durability, GFRP is a widely used material for a number of applications [11]. It is frequently utilised for lightweight components in the aerospace and automotive industries as well as for reinforcing concrete structures including bridges, tunnels, and buildings. GFRP is commonly manufactured by laying sheets of glass fibres in a mould, soaking the fibres in resin, and letting the resin to cure. The resulting composite material is adaptable for a wide range of applications since it can be moulded into a variety of shapes and sizes.

Chopped Strand Mat (CSM) form of reinforcing material is constructed from short glass fibre strands that are randomly oriented and bound together with a binder. The glass fibres are chopped into continuous strands that are between one and two inches long. The manufacture of composite materials frequently makes use of CSM, particularly in hand lay-up and spray-up procedures. In order to bind the fibres together and create a solid composite part, the material is typically placed in a mould and coated with resin [12, 13]. Using CSM has benefits like as inexpensive cost, simplicity of handling, and good conformability to complex geometries. CSM application includes in the marine, automotive, and construction industries, and it is also compatible with a wide range of resins. CSM also have certain drawbacks as well. In comparison to other reinforcing materials like woven fabrics or unidirectional fibres, it may have lower mechanical properties and be more challenging to achieve consistent fibre orientation. Furthermore, CSM frequently has a rough surface finish, necessitating extra surface preparation or finishing operations. The flexural strength of RC components can be increased by using FRP laminates. The mechanical integrity of RC beams enhanced by hybridization of CSM and GFRP of various thicknesses for flexure has received less research. The experiments were performed on the RC beams strengthened with FRP composite wrapping on three sides in order to increase their load carrying capacity, stiffness, and ductility. All RC beams are constructed from M30 grade concrete. For flexure, all five beams used a four-point bending strategy [14].

PERIQUITO *et al.* [15] concludes that crushed stone sand can be used as an alternative to natural sand in steel fiber reinforced concrete. The total substitution of natural sand for sand manufactured from crushed stone decreases the compressive and bending strength but significantly increases abrasion resistance. However, the elastic modulus of the mixtures remains approximately equal. The use of 100% stone powder content reduces the cost of production by about 32%. OLIVEIRA JÚNIOR *et al.* [16] presents an analytical model for stress-strain curve for steel fiber-reinforced concrete, which was derived for concretes with strengths of 40 MPa and 60 MPa at the age of 28 days. The accuracy of the proposed stress-strain curve was evaluated by comparison of the area under stress-strain curve, and the results showed good agreement between analytical and experimental data and the benefits of using fibers in the compressive behavior of concrete. PALANIAPPAN *et al*. [17] investigates the use of functionally graded concrete (FGC) by using red mud and fly ash as alternative materials. The study concludes that FGC has more durability and strength characteristics than ordinary concrete. KARUPPANAN *et al.* [18] concludes that the newly developed hybrid fiber reinforced concrete-filled steel tubular sections display significant improvement in the flexural performance. The study also suggests that the optimum fiber dosage in each fiber type can be determined based on the performance of mono fiber reinforced concrete mixes. The results of the study can be useful in the design of concrete-filled steel tubular structures.

While there is a growing body of research on the use of FRP laminates in reinforcing concrete beams, limited studies have focused specifically on the structural performance of hybrid FRP laminates in conjunction with concrete beams made using manufactured sand. Although manufactured sand is increasingly being utilized as a sustainable alternative to natural sand in concrete production, its interaction with hybrid FRP laminates remains relatively unexplored. Understanding the structural behavior and performance of hybrid FRP laminates on concrete beams incorporating manufactured sand is essential for optimizing their application in real-world engineering projects. The research focuses on exploring the structural performance of hybrid FRP laminates when applied to concrete beams made with manufactured sand. The objectives are to assess flexural performance compared to steel-reinforced beams, analyze failure modes under various loading conditions, evaluate load-deflection responses for ductility and energy absorption capacity, compare structural performance with conventional steel-reinforced beams, and investigate long-term durability and resistance to corrosion. The study aims to provide insights into the effectiveness of hybrid FRP laminates in reinforcing manufactured sand concrete beams, contributing to sustainable and resilient construction practices.

2. MATERIALS AND METHODS

The concrete used in this study adheres to the specifications outlined in IS12269:2013, with cement as the binding material. The fine aggregate is obtained from river sand, while the coarse aggregate meets the requirements set forth in IS 383:2016. To investigate the effects of various additives, the concrete mix incorporates manufactured sand (M-Sand) in increments of 5% up to a maximum of 40%. Fly ash, which acts as a viscosity modifier, is included according to the guidelines specified in IS3812 (Part1) 2013. Additionally, steel and glass are added to the mix in increments of 0.5% up to a maximum of 2%. The properties of these additives are detailed in the accompanying tables. The addition of steel and glass in concrete serves to enhance its mechanical properties & overall performance. Resulting in improved strength, toughness, and crack control. It exhibits increased tensile and flexural strength, reducing the likelihood of cracking and enhancing its durability. The use of steel and glass offers ease of construction and makes it a handy material in various applications, such as industrial flooring, precast elements, tunnel linings, concrete repairs.

2.1. Concrete

According to IS 10262: 2019 and IS 456:2000, the target compressive strength of 38.50 MPa for the concrete mix was established for 28 days of curing. All casting batches were completed in accordance with the mix design created in the lab through the use of material tests. In the final mix design parameters, which are all given in kg/m3 as weigh batching, cement, fine and coarse aggregate is equal to 385, 675 and 1206 respectively, water is equal to 154, and superplasticizer is equal to 3.90. After casting, the beams underwent a 28-day water cure. To evaluate the strength properties, other specimens such cubes, prisms, and cylinders were also cast and tested.

2.2. Steel reinforcement bar and fiber reinforced polymer laminates

High Yield Strength Deformed (HYSD) reinforcing bars of the Fe500 grade were used. Unidirectional E-glass and chopped strand mat were used in this work. Hand layup is the method used to create FRP laminates. Isophthalic polyester resin and a hardener bond individually. (Resin: Hardener 1:10) to form laminates. In this work, externally bonded FRP strengthening was accomplished using FRP laminates with dimensions of 3000 mm × 150 mm.

Table 1: Properties of isophthalic polyester resin.

TESTS	VALUES	LIMITS
Colour	Light yellow	–
Specific gravity @ 27˚C	1.12	1.1–1.25
Viscosity	140 seconds	120–160 seconds
Volatile content	37%	30–38%
Acid value	13.2 mg KOH/g	9–15 mg KOH/g
Gel time @ 29˚C	8 Minutes	8–15 Minutes
Peak temperature	192˚C	165˚C–195˚C

Source: Manufacturer.

2.3. Isophthalic polyester resin

Epoxy resin with a hardener was used for bonding FRP laminates to the concrete surface. Table 1 lists the resin characteristics.

3. EXPERIMENTAL TEST PROGRAM

In order to determine the optimal percentage of M-sand replacement, strength experiments were conducted and the results were obtained and optimized. To address the challenges of conducting numerous trials and minimizing material wastage, the RSM was employed as an analytical tool. It utilizes the CCD to predict the ideal dosage of ingredients and validate it against experimental results. By using RSM and CCD, the optimum replacement percentage of M-sand in the concrete mixes can be determined. This approach reduces the number of trials required, saving time and resources (Table 2). It provides valuable insights into the relationship between variables and response, aiding in the optimization of strength and durability properties. Strength properties were assessed on concrete specimens by conducting tests on compressive, split tensile and flexural strength values on 7 and 28 days of curing.

3.1. Details of specimens

Experimental investigation carried out on five simply supported beams with a total length of 3000 mm, a span length of 2800 mm, a depth of 250 mm, and a breadth of 150 mm. These beams are shown in Figure 1. All of the beams were reinforced with two 8 mm diameter steel reinforcing bars utilised as closed loop stirrups at a spacing of 150 mm and two 10 mm diameter compression and tension reinforcement bars. The beams were under-reinforced portions and were designed utilising the limit state technique of design as stated in IS 456:2000.

This experimental programme involves testing RC beams with and without FRP strengthening, as shown in Table 1. One conventional, unstrengthened beam was evaluated, while the other four beams were reinforced with FRP composite laminates. The details of RC beam specimens in Table 3.

3.2. Casting and curing

The test programme included the casting and testing of a total of five beams. One beam was the control, while the other four were strengthened using four different FRP laminates. Five beams were cast with a reinforcement ratio of 0.419%. (wrapping of the beam). All five beams were reinforce using two 10 mm steel bars, one for tension and the other for compression. The beam samples were cast using the wooden moulds. Tie wires were used to construct steel reinforcing cages for each specimen. A gang casting was used to place the required quantity of concrete. Oil was applied to the interior of the moulds to prevent concrete from sticking to it. To avoid honeycombing, the concrete was thoroughly vibrated after being correctly poured in layers. After casting for 24 hours, the beam specimens were unmolded and given 28 days to water cure. Figure 2 depicts the casting process.

3.3. RC beam external strengthening procedure

Reinforced Concrete (RC) beam external strengthening, also known as concrete beam strengthening or retrofitting, is a structural strengthening technique used to enhance the load-carrying capacity and durability of existing RC beams. This technique is commonly employed in situations where the original beams exhibit signs of distress, inadequate load-carrying capacity, or when there is a need to upgrade the structure to accommodate higher loads or new design requirements. External strengthening methods involve adding additional materials

Table 2: Details of test program.

MIX ID	M-SAND REPLACEMENT (%)	MIX ID	PERCENTAGE ADDITION	
			STEEL	GLASS
MS0	0	HF0.5:0.5	0.5	0.5
MS05	5	HF0.5:1.0	0.5	1.0
MS10	10	HF0.5:1.5	0.5	1.5
MS15	15	HF0.5:2.0	0.5	2.0
MS20	20	HF1.0:0.5	1.0	0.5
MS25	25	HF1.0:1.0	1.0	1.0
MS30	30	HF1.0:1.5	1.0	1.5
MS35	35	HF1.0:2.0	1.0	2.0
MS40	40	HF1.5:0.5	1.5	0.5
		HF1.5:1.0	1.5	1.0
		HF1.5:1.5	1.5	1.5
		HF1.5:2.0	1.5	2.0
		HF2.0:0.5	2.0	0.5
		HF2.0:1.0	2.0	1.0
		HF2.0:1.5	2.0	1.5
		HF2.0:2.0	2.0	2.0

Figure 1: Steel reinforcing details.

Table 3: Details of RC beam specimens.

BEAM DESIGNATION	STRENGTHENED FRP TYPE	COMBINATION OF FIBER, %
B	–	–
BH1	CSM + G	1 layer of CSM & 1 layer of GFRP
BH2	CSM + 2G	1 layer of CSM & 2 layers of GFRP
BH3	CSM + 3G	1 layer of CSM & 3 layers of GFRP
BH4	CSM + 4G	1 layer of CSM & 4 layers of GFRP

and layers externally to the beam's surface to improve its performance. FRP composites are externally bonded to the concrete beam using epoxy resins. FRP strengthening provides enhanced tensile strength, flexural strength, and ductility to the beam, reducing cracking and increasing its load-carrying capacity. After curing, the process of reinforcing the beams was carried out. According to the guidelines in ACI 440.2R, the external flexural bonding strengthening of RC beams wrapping using FRP laminates was completed. The surfaces are cleaned with a grinding machine before the FRP sheet is fastened to the beam. In order to wrap the FRP laminates (using a hand layup procedure carried out on site) and keep them on the final resin matrix using a roller, a uniformly thick coating of adhesive is first placed to the concrete surfaces. Dead loads were applied on the concrete surface, allowed to dry for 4–6 days, and then tested to ensure a solid bond formed between the FRP laminates and the concrete. The methodological procedure used for external strengthening is depicted in Figure 3.

Figure 2: Casting of beam specimens.

Figure 3: a) Surface treatment and b) strengthened beam process.

Figure 4: Details of the beam during testing.

3.4. Test setup

The tested beams had straight forward supported with a bearing of roughly 100 mm and an effective span length of 2800 mm, as shown in Figure 4. RC beams subjected to four-point bending were examined utilizing a reaction-type 500 kN in loading frame. A longitudinal stiff steel spreader beam was used to distribute the load cell's weight to the beams. End supports consist of a roller and a hinge that allowed end rotation. To understand the fracture propagation and failure pattern, crack marking was performed throughout the testing process at intervals of 5 kN of loading to measure the deflection of the beam, dial gauges were positioned at both the midspan and the location where the load was applied.

4. RESULTS AND DISCUSSION

4.1. Experimental optimization on strength properties

Strength properties of materials are typically determined through laboratory experiments. In the context of concrete, several tests are commonly conducted to assess its strength. The most common test is the compressive strength test, which measures the maximum load a material can withstand before failure under compression. The compressive strength values range from 18.16 MPa to 22.70 MPa at 28 days of curing [19]. As the percentage of M-sand increases from 0% to 25%, the compressive strength generally improves. However, the mix with 30% m-sand shows a slight decrease in compressive strength compared to the previous mix. This suggests that there might be an optimal range of M-sand content for achieving the highest compressive strength (Table 4). The split tensile strength values range from 2.72 MPa to 3.00 MPa at 28 days of curing. Similar to compressive strength, the split tensile strength generally increases with increasing percentages of M-sand, except for the mix with 30% M-sand which shows a lower value (Table 5). The flexural strength values range from 3.26 MPa to 4.81 MPa at 28 days of curing. The trend in flexural strength follows a similar pattern to the compressive and split tensile strength, showing an improvement with increasing percentages of M-sand [20].

Table 4: Effect of M-sand.

MIX ID	COMPRESSIVE STRENGTH (MPa)		SPLIT TENSILE (MPa)		FLEXURAL STRENGTH (MPa)	
	7	28	7	28	7	28
MS0	18.44	33.62	2.73	3.47	3.28	4.37
MS05	19.23	34.96	2.78	3.53	3.34	4.45
MS10	20.14	36.29	2.84	3.60	3.41	4.53
MS15	21.00	37.55	2.90	3.65	3.48	4.60
MS20	21.49	39.06	2.93	3.72	3.52	4.69
MS25	22.70	41.23	3.00	3.82	3.61	4.81
MS30	20.72	37.71	2.88	3.66	3.46	4.61
MS35	19.65	35.79	2.81	3.57	3.38	4.50
MS40	18.16	33.11	2.72	3.45	3.26	4.34

Table 5: Effect of hybrid combinations.

MIX ID	COMPRESSIVE STRENGTH (MPa)		SPLIT TENSILE (MPa)		FLEXURAL STRENGTH (MPa)	
	7	28	7	28	7	28
HF0.5:0.5	27.11	42.38	3.25	3.87	3.92	4.87
HF0.5:1.0	27.28	42.63	3.25	3.88	3.93	4.88
HF0.5:1.5	27.56	43.05	3.27	3.90	3.95	4.91
HF0.5:2.0	27.96	43.67	3.29	3.92	3.97	4.94
HF1.0:0.5	27.61	43.14	3.27	3.90	3.95	4.91
HF1.0:1.0	27.91	43.60	3.29	3.92	3.97	4.93
HF1.0:1.5	29.26	45.14	3.51	4.07	4.09	5.14
HF1.0:2.0	28.44	44.41	3.32	3.96	4.00	4.98
HF1.5:0.5	28.38	44.32	3.31	3.95	4.00	4.97
HF1.5:1.0	28.40	44.35	3.31	3.95	4.00	4.97
HF1.5:1.5	28.56	44.60	3.32	3.96	4.01	4.99
HF1.5:2.0	28.47	44.45	3.32	3.96	4.01	4.98
HF2.0:0.5	28.51	44.53	3.32	3.96	4.01	4.98
HF2.0:1.0	28.40	44.34	3.31	3.95	4.00	4.97
HF2.0:1.5	28.24	44.10	3.31	3.94	3.99	4.96
HF2.0:2.0	28.15	43.96	3.30	3.94	3.99	4.95

Most of the concrete mixes, achieved the desired level of target strength with the replacement of M-sand. This means that the concrete mixes were able to create with the help of M-sand without compromising the strength properties. The inclusion in all combinations resulted in improved strength parameters compared to conventional concrete. The specific combinations were found to be effective for enhancing strength varied based on the mix design and experimental conditions [21, 22]. Considering the strength parameters and workability considerations, it was concluded that the optimal volume fraction addition of 1.0% steel and 1.5% glass with a M-sand replacement of 25%.

4.2. Statistical optimization of strength properties

Design Expert, developed by Stat-Ease Inc., is a specialized statistical software package designed for conducting experimental design (DOE). It offers a range of features such as comparison testing, screening, characterization, optimization, robust parameter design, mix designs, and combined designs. With Design Expert, users can assess the statistical significance of factors through analysis of variance (ANOVA). The software provides graphical tools that enable users to visualize the impact of each factor on the desired outcomes and identify any inconsistencies in the data. In the context of Central Composite Design (CCD), the number of experimental runs is determined by multiplying the number of levels for numerical factors by the number of combinations for categorical factors. When two categorical factors with three levels each are introduced, the total number of runs is multiplied by 9. Optimal designs often incorporate a combination of numerical and categorical factors. In this investigation, Central Composite Design (CCD) was utilized for optimizing concrete ingredients, offering significant advantages over other methods. CCD enables efficient exploration of the factor space by systematically varying the proportions of concrete ingredients. This design reduces the number of experimental runs required compared to a full factorial design, resulting in time, resource, and cost savings. The inclusion of star points in CCD allows for the assessment of nonlinearity and interactions between ingredients using statistical techniques like regression analysis and analysis of variance (ANOVA) for data analysis. The response surface model obtained from CCD provides a mathematical representation of the system, facilitating predictions and optimization of ingredient proportions beyond the experimental design space. Engineers and researchers can leverage these models to estimate optimal ingredient proportions and explore various scenarios without the need for additional experiments. The input data for the CCD approach in Design Expert software is presented in Table 6.

Table 6: Input data for CCD approach in design expert.

STD	RUN	A: M-SAND %	B: STEEL %	C: GLASS %	RESPONSE: COMPRESSIVE STRENGTH (MPa)
7	4	20	1.5	2	42.27
9	6	20	1	1.5	44.17
5	8	20	0.5	2	43.24
3	10	20	1.5	1	44.73
1	16	20	0.5	1	41.19
19	1	25	1	1.5	45.14
13	3	25	1	1	44.23
14	5	25	1	2	43.62
20	7	25	1	1.5	45.27
16	9	25	1	1.5	45.36
11	11	25	0.5	1.5	44.85
17	14	25	1	1.5	44.96
12	15	25	1.5	1.5	43.75
18	17	25	1	1.5	45.24
15	18	25	1	1.5	45.59
4	2	30	1.5	1	44.05
2	12	30	0.5	1	43.21
10	13	30	1	1.5	42.76
6	19	30	0.5	2	41.94
8	20	30	1.5	2	40.73

The customization summary provides essential statistics that assist in choosing the appropriate starting point for the final model selection. The Whitcomb Score is used to identify the preferred models. It is important to note that the proposed model should be viewed as a favorable initial point for model adaptation [23]. The Design Expert software was utilized to incorporate the input factors, and Table 7 presents a comprehensive summary of these factors.

Three input factors are considered: M-Sand replacement, Steel percentage, and Glass percentage. M-Sand replacement ranges from 20% to 30%, Steel percentage varies from 0.5% to 1.5%, and Glass percentage ranges from 1% to 2%. Each factor is represented in coded units, ranging from –1 to +1, with their corresponding minimum and maximum values. The mean and standard deviation of each factor are provided as well. The output response is the compressive strength of the concrete, measured in MPa. The study collected 20 observations and conducted a polynomial analysis. The compressive strength ranges from 40.73 MPa to 45.59 MPa, with a mean value of 43.82 MPa and a standard deviation of 1.44 MPa.

The transformation of the response is an important part of any data analysis. A transformation is required if the error is a function of the size of the response. Design Expert provides in-depth diagnostics to ensure that the statistical assumptions underlying the data analysis are met. The normal representation of the residues tests their normality [24–27]. The representation of the residual and predicted values of the response indicates a problem if there is a pattern. If the ratio between the minimum and maximum responses is not large, the transformation of the response does not make much difference (Table 8).

Table 7: Input and output factors in fit summary.

INPUT FACTORS									
FACTOR	**NAME**	**UNITS**	**TYPE**	**MINIMUM**	**MAXIMUM**	**CODED LOW**	**CODED HIGH**	**MEAN**	**STD. DEV.**
A	M-Sand replacement	%	Numeric	20.00	30.00	–1 ↔ 20.00	+1 ↔ 30.00	25.00	3.63
B	Steel	%	Numeric	0.5000	1.50	–1 ↔ 0.50	+1 ↔ 1.50	1.0000	0.3627
C	Glass	%	Numeric	1.0000	2.00	–1 ↔ 1.00	+1 ↔ 2.00	1.50	0.3627
OUTPUT RESPONSE									
RESPONSE	**NAME**	**UNITS**	**OBSERVATIONS**		**ANALYSIS**	**MINIMUM**	**MAXIMUM**	**MEAN**	**STD. DEV.**
R1	Compressive Strength	MPa	20		Polynomial	40.73	45.59	43.82	1.44

Table 8: Analysis of variance.

SOURCE	SUM OF SQUARES	df	MEAN SQUARE	F-VALUE	p-VALUE	
Model	35.53	9	3.95	10.84	0.0004	significant
A-M-Sand replacement	0.8468	1	0.8468	2.32	0.1584	
B-Steel	0.1210	1	0.1210	0.3321	0.5772	
C-Glass	3.15	1	3.15	8.64	0.0148	
AB	1.08	1	1.08	2.97	0.1158	
AC	2.18	1	2.18	5.99	0.0344	
BC	5.38	1	5.38	14.76	0.0033	
A^2	4.29	1	4.29	11.79	0.0064	
B^2	0.4726	1	0.4726	1.30	0.2813	
C^2	1.71	1	1.71	4.71	0.0552	
Residual	3.64	10	0.3643			
Lack of Fit	3.42	5	0.6839	15.28	0.0047	significant
Pure Error	0.2238	5	0.0448			
Cor Total	39.18	19				

The Model F-value of 10.84 implies the model is significant. There is only a 0.04% chance that an F-value this large could occur due to noise. P-values less than 0.0500 indicate model terms are significant. In this case C, AC, BC, A^2 are significant model terms. Values greater than 0.1000 indicate the model terms are not significant. If there are many insignificant model terms (not counting those required to support hierarchy), model reduction may improve your model. The Lack of Fit F-value of 15.28 implies the Lack of Fit is significant. There is only a 0.47% chance that a Lack of Fit F-value this large could occur due to noise. Significant lack of fit is bad – we want the model to fit (Figure 5).

$$\text{Compressive Strength} = -8.47541 + 2.90139A + 12.13136B + 16.85755C - 0.147000AB - 0.209000AC - 3.28000BC - 0.049982A^2 - 1.65818B^2 - 3.15818C^2$$

The equation in terms of real factors can be used to predict the response for given levels of each factor [28]. Here, the levels must be specified in the units of origin for each factor. This equation should not be used to determine the relative impact of each factor because the coefficients are scaled to account for the units of each factor and the intercept is not in the center of the space of the design space [29].

As for the reason for a red color dot in the figure, it is essential to consider the context of the study and the experimental design. In many cases, a red color dot in a figure can represent an outlier or an observation that falls outside the expected or typical range of data points. Design Expert software offers a range of graphical tools to aid in the interpretation of the selected model. These visualizations can be accessed by adjusting a template and clicking on the Graphic Model button. In factorial designs, the key graphs include the single factor, interaction, and cube plots. The single factor chart allows for the examination of the main effects of factors that are not involved in an interaction. The interaction graph displays two-factor interactions. The cube plot provides a visualization of the relationship between three factors. For Response Surface and Mixing designs, the primary graphs of interest are the outline and 3D surface plots (Figure 6). These graphs enable users to analyze the response surface and visualize the impact of factors on the desired outcomes. The point forecast allows the analyst to define factor values [30–33]. Models are used to provide forecasts and interval estimates. The confirmation compares the prediction interval of the model with the average of a subsequent sample. If the average value of the samples is in the prediction interval, the model is confirmed. Confirmation generally corresponds to near or close factor parameters recommended by numerical optimization. The coefficient table indicates the size and significance of the coefficients for all analyzed responses. It is color-coded according to its importance. Facilitates the recognition of terms common to all response models. Figure 7 shows the optimized parameters from design expert software and it was taken by point prediction analysis [34].

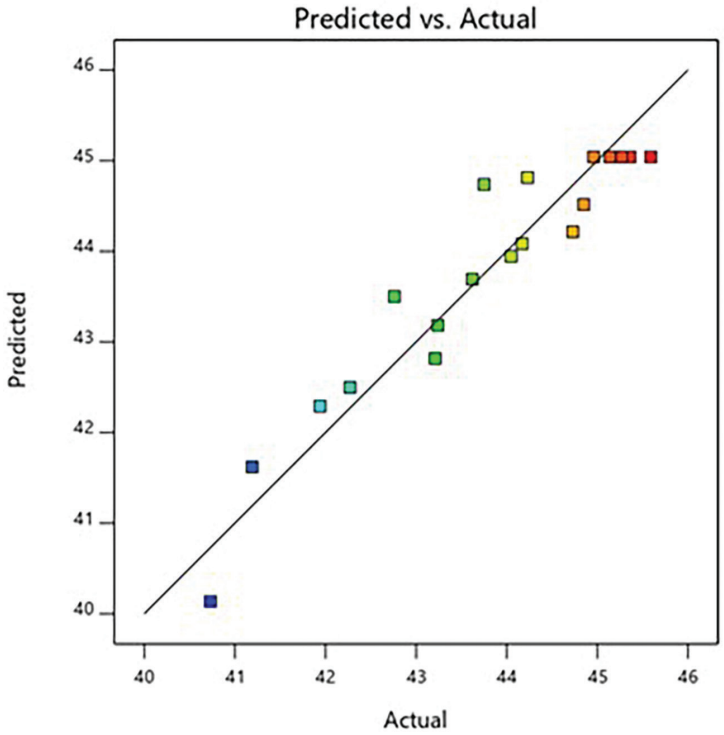

Figure 5: Predicted vs actual graph on compressive strength prediction.

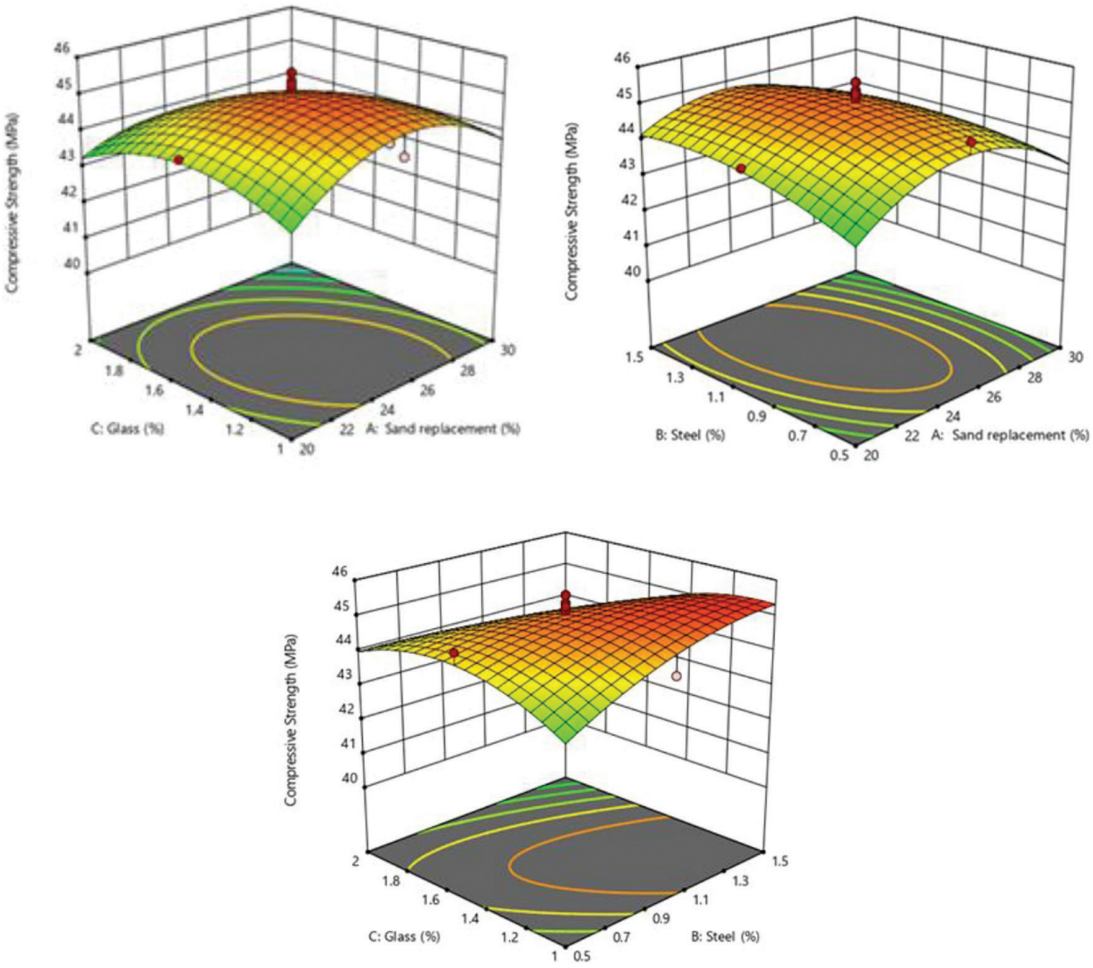

Figure 6: 3D contour plots from RSM.

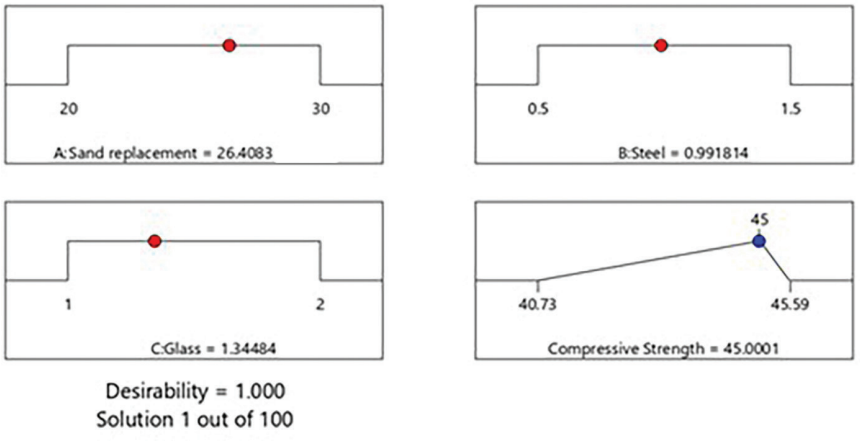

Figure 7: Statistical optimization of input parameters.

Statistically optimized ingredients have produced a compressive strength of 47.17 MPa at 28 days of curing, exceeding the target strength of 38.5 MPa. The success is attributed to careful selection and proportioning of materials, improved material properties, enhanced curing process, and reduction of weak points. Statistical optimization reduces variability and considers interactions between ingredients, prioritizing strength

as a primary objective in the mix design. As a result, the concrete mix achieved a stronger and more consistent compressive strength. From the observed data from point prediction analysis, it was concluded that, statistically optimized ingredients can produce compressive strength of 47.17 MPa at 28 days of curing which was 4.5% greater than the specimens made with experimentally optimized [35, 36]. By considering the strength properties, statistically optimized ingredients were utilized in the further stages of the investigation.

4.3. Load-displacement performance of RC beam

The beam (B) ultimate load deflected by 27.36 mm at the midspan, or 41 kN. The strengthened control beam (BH3) had a midspan deflection of 39.08 mm and the highest maximum load of the five beams at 107 kN, or a 160.97% increase in load carrying capacity, over the control beam (B). The strengthened beams were more ductile. The FRP sheeted beam (BH4) demonstrated sheet separation from the concrete surface and had a lower load carrying capability of 85 kN when compared to the strengthened beams [37]. The ultimate load behaviour and ultimate deflection of RC unstrengthen and strengthened beams are shown in Figures 8 and 9.

4.4. Mode of beam failure

Under loads between 22 and 34 kN, the bottom side and in the direction of the compression side in the moment zone, all five specimens experienced the first vertical crack. The constant moment zone then developed sporadic flexural stress cracks. The beams have a fair amount of ductility before breaking under flexure. The impetus

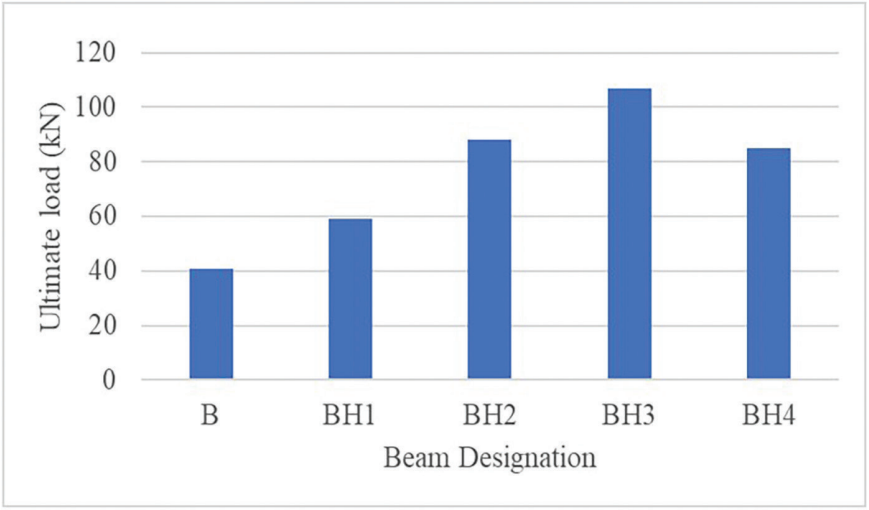

Figure 8: Ultimate load of unstrengthen and strengthened RC beams.

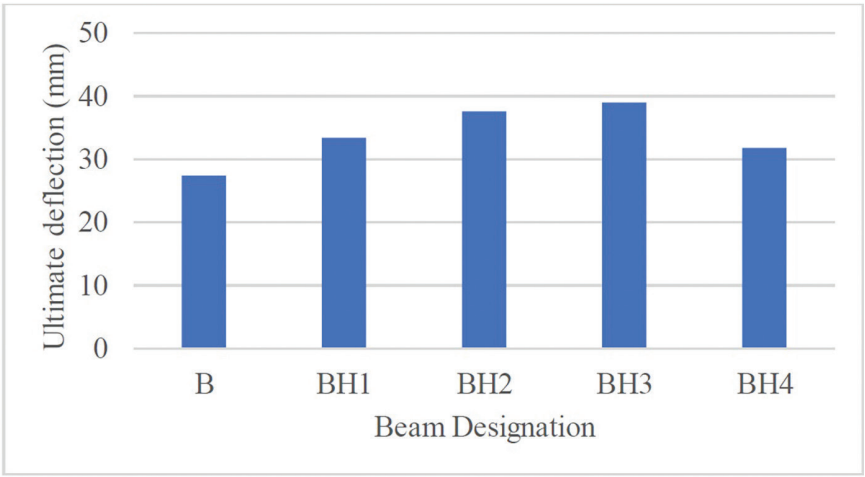

Figure 9: Ultimate deflection of unstrengthen and strengthened RC beams.

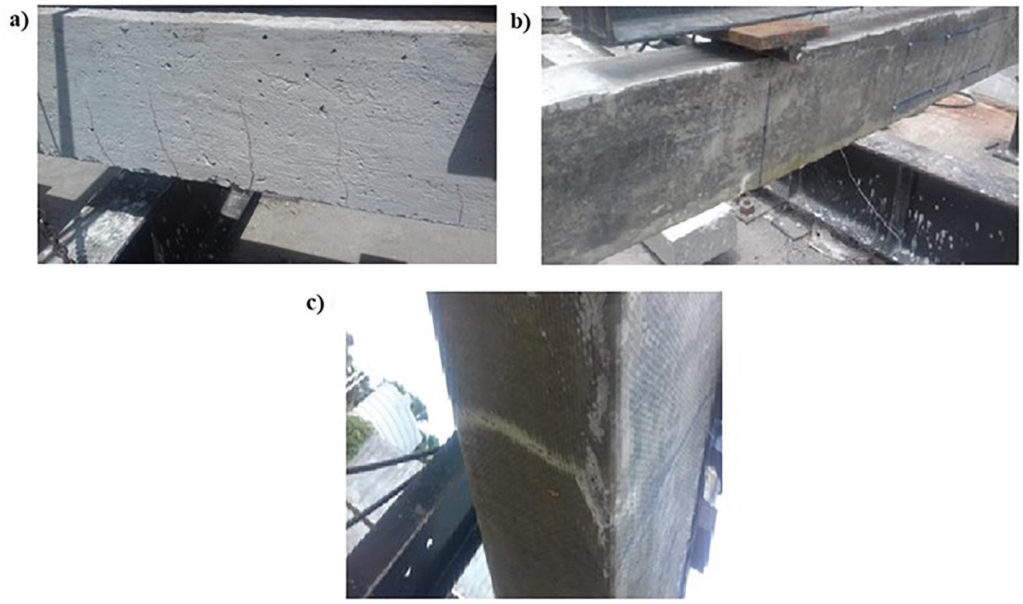

Figure 10: Failure mechanisms of beams. a) controlled beam b) BH2 and c) BH3.

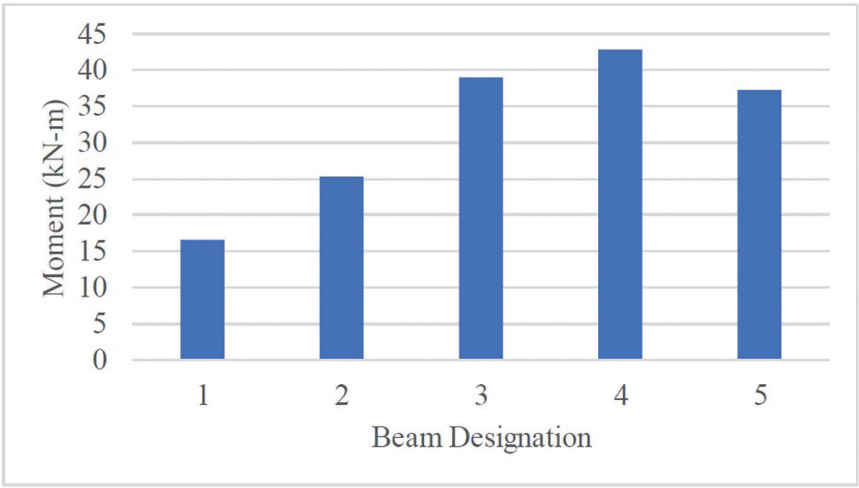

Figure 11: Moment behavior of unstrengthen and strengthened RC beams.

for the failure mode of the reinforced beam was the multiple crack formation on the tension side [38, 39]. The laminates restraining effect on the crack opening prevented it from widening during the course of the loading procedure, and it remained narrower than the cracks in the control beams. More cracks started to show up along the shear span as a result of the larger loading section. The control beam demonstrated flexural failure, as shown in Figure 10.

4.5. Moment-curvature behavior

Figure 11 compares the moment-curvature behaviour of RC beams based on the experiment data. The moment capacity, which determines the beam's resistance to rotation when it is loaded, is a key flexure parameter. The specimen's curvature, which is used to explain how the beam bends, is determined by how eccentric the specimen is from its normal plane after loading. Dial gauges are positioned in the compression and tension areas of the beam to monitor displacement, which was then converted into strain values to determine the curvature of the beam. The curvature at failure was improved by FRP strengthening, though (Table 9).

The energy absorption capacity of RC beams is a crucial characteristic that indicates their ability to absorb and dissipate energy during loading and deformation. This capacity is closely related to the beam's ductility and

Table 9: Optimization of results.

EXPERIMENTALLY OPTIMIZED		STATISTICALLY OPTIMIZED	
INGREDIENTS	**VALUES**	**INGREDIENTS**	**VALUES**
M-Sand	25%	M-Sand	26.41%
Steel	1%	Steel	0.99%
Glass	1.5%	Glass	1.34%
Compressive Strength	45.14 MPa	Compressive Strength (Expected)	45 MPa
		Compressive Strength (Observed)	47.17 MPa

Table 10: Parameters results obtained from test.

PARAMETERS	B	BH1	BH2	BH3	BH4
Ultimate load (kN)	41	59	88	107	85
Ultimate deflection (mm)	27.36	33.51	37.72	39.08	31.89
Moment (kN-m)	17.72	35.92	43.38	53.65	41.99

toughness, which are vital for ensuring the structure's safety and resilience. Several factors influence the energy absorption capacity, including material properties, cross-sectional geometry, reinforcement details, load and boundary conditions, concrete cover, and confinement [40, 41]. Properly designed and well-distributed reinforcement, along with adequate concrete cover, enhances the beam's ability to resist cracking and deformation, resulting in higher energy absorption (Table 9). Achieving an optimal balance between strength, stiffness, and ductility is essential in structural design to ensure the beams can effectively absorb and dissipate energy without sudden failure, making them suitable for earthquake-resistant structures.

The investigation on the structural performance of hybrid FRP laminates on concrete beams made with manufactured sand provides several benefits. It promotes sustainable construction by exploring the use of eco-friendly manufactured sand. The study optimizes material utilization, leading to cost-effective construction while maintaining structural integrity. Additionally, it highlights the potential of hybrid FRP laminates to enhance mechanical properties and increase resilience [42, 43]. The investigation improves durability and corrosion resistance, encourages broader use of FRP materials in civil engineering, and contributes to advancing knowledge in the field [44].

5. CONCLUSIONS

The results of five RC beams that were experimentally wrapped in FRP laminates and reinforced. Following a review of the effectiveness of the suggested strengthening strategy, the following results are reached:

- The results suggested that utilizing environmentally friendly materials like M-sand, in conjunction with advanced FRP technologies, not only improves strength and structural performance but also aligns with the principles of sustainable construction, reducing the industry's ecological footprint.
- RSM is an effective technique for the statistical optimization process. Statistically optimized ingredients can produce compressive strength of 47.17 MPa at 28 days of curing which was 4.5% greater than the specimens made with experimentally optimized.
- In comparison to the control beam, the strengthened RC beams displayed more notable flexural capacity findings (B). The findings suggest that the combined use of different types of FRP materials will significantly improve the load-carrying capacity and overall durability of concrete beams, particularly when manufactured sand is employed in their composition.
- BH1, BH2, and BH3 FRP laminate enhanced beams, and energy absorption capacity rose significantly. The strengthened beam (BH3) had a greater rise load-carrying capability of 115 kN than the unstrengthen beam.
- The study concluded that RC beams strengthened with FRP sheets may support concrete constructions. The utilization of FRP composites, particularly the successful application of laminates, holds promise for revitalizing existing structures and potentially redefining the future of construction methods for increased resilience and longevity.

6. BIBLIOGRAPHY

[1] AI-HUI, Z., WEI-LIANG, J., GUI-BING, L., "Behaviour of preloaded RC beams strengthened with CFRP laminates", *Journal of Zhejiang University. Science A*, v. 7, n. 3, pp. 436–444, 2006. doi: http://dx.doi.org/10.1631/jzus.2006.A0436

[2] ESFAHANI, M., KIANOUSH, M., TAJARI, A., "Flexural behaviour of reinforced concrete beams strengthened by CFRP sheets", *Engineering Structures*, v. 29, n. 10, pp. 2428–2444, 2007. doi: http://dx.doi.org/10.1016/j.engstruct.2006.12.008

[3] PHAM, H., AL-MAHAIDI, R., "Experimental investigation into flexural retrofitting of reinforced concrete bridge beams using FRP composites", *Composite Structures*, v. 66, n. 1–4, pp. 617–625, 2004. doi: http://dx.doi.org/10.1016/j.compstruct.2004.05.010

[4] TENG, J.G., ZHANG, J.W., SMITH, S.T., "Interfacial stresses in reinforced concrete beams bonded with a soffit plate: a finite element study", *Construction & Building Materials*, v. 16, n. 1, pp. 1–14, 2002. doi: http://dx.doi.org/10.1016/S0950-0618(01)00029-0

[5] SPADEA, G., SWAMY, R.N., BENCARDINO, F., "Strength and ductility of rc beams repaired with bonded CFRP laminates", *Journal of Bridge Engineering*, v. 6, n. 5, pp. 349–355, 2001. http://dx.doi.org/10.1061/(ASCE)1084-0702(2001)6:5(349)

[6] RAHIMI, H., HUTCHINSON, A., "Concrete beams strengthened with externally bonded FRP plates", *Journal of Composites for Construction*, v. 5, n. 1, pp. 44–56, 2001. doi: http://dx.doi.org/10.1061/(ASCE)1090-0268(2001)5:1(44)

[7] ZHANG, A., JIN, W., LI, G. "Behaviour of preloaded RC beams strengthened with CFRP laminates", *Journal of Zhejiang University*, v. 7, n. 3, pp. 436–444, 2006. doi: http://dx.doi.org/10.1631/jzus.2006.A0436

[8] KHURI, A.I., MUKHOPADHYAY, S., "Response surface methodology", *Wiley Interdisciplinary Reviews: Computational Statistics*, v. 2, n. 2, pp. 128–149, 2010. doi: http://dx.doi.org/10.1002/wics.73

[9] KIM, H.S., SHIN, Y.S., "Flexural behavior of reinforced concrete (RC) beams retrofitted with hybrid fiber reinforced polymers (FRPs) under sustaining loads", *Composite Structures*, v. 93, n. 2, pp. 802–811, 2011. doi: http://dx.doi.org/10.1016/j.compstruct.2010.07.013

[10] NASER, M., HAWILEH, R., ABDALLA, J.A., *et al*., "Bond behavior of CFRP cured laminates: experimental and numerical investigation", *Journal of Engineering Materials and Technology*, v. 134, n. 2, pp. 021002, 2012. doi: http://dx.doi.org/10.1115/1.4003565

[11] CARLEY, K.M., KAMNEVA, N.Y., REMINGA, J. (2004). *Response surface methodology*, Pittsburgh, Carnegie-Mellon Univ. doi: http://dx.doi.org/10.21236/ADA459032

[12] FATHELBAB, F.A., RAMADAN, M.S., AL-TANTAWY, A., "Strengthening of RC bridge slabs using CFRP sheets", *Alexandria Engineering Journal*, v. 53, n. 4, pp. 843–854, 2014. doi: http://dx.doi.org/10.1016/j.aej.2014.09.010

[13] ISKANDER, M., EL-HACHA, R., SHRIVE, N., "Governing failure criterion of short-span hybrid FRP-UHPC beams subjected to high shear forces", *Composite Structures*, v. 185, pp. 123–131, 2018. doi: http://dx.doi.org/10.1016/j.compstruct.2017.11.003

[14] BAŞ, D., BOYACI, I.H., "Modeling and optimization I: usability of response surface methodology.", *Journal of Food Engineering*, v. 78, n. 3, pp. 836–845, 2007. doi: http://dx.doi.org/10.1016/j.jfoodeng.2005.11.024

[15] PERIQUITO, M.D. S., & MAGALHÃES, M. D. S. (2017). "Mechanical behaviour of steel fiber reinforced concrete with stone powder", *Matéria (Rio de Janeiro),* v. 22, n.2, pp. 1–7, 2017. doi: https://doi.org/10.1590/S1517-707620170002.0172

[16] OLIVEIRA JÚNIOR, L.Á.D., BORGES, V.E.D.S., DANIN, A.R., MACHADO, D.V.R., ARAÚJO, D.D.L., EL DEBS, M.K., & RODRIGUES, P.F. "Stress-strain curves for steel fiber-reinforced concrete in compression", *Matéria (Rio de Janeiro),* v.15, n.2, pp.260–266, 2010. doi: https://doi.org/10.1590/S1517-70762010000200025.

[17] PALANIAPPAN, S.M., GOVINDASAMY, V., & JABAR, A.B. "Experimental investigation on flexural performance of functionally graded concrete beams using flyash and red mud". *Matéria (Rio de Janeiro),* v.26, n. 1, pp.1–11, 2021. doi: https://doi.org/10.1590/S1517-707620210001.1213

[18] KARUPPANAN, K., & GOVINDASAMY, V. "Behaviour of hybrid fibre reinforced concrete-filled steel tubular beams and columns". *Matéria (Rio de Janeiro),* v.25, n.1, pp.1–12, 2020. doi: https://doi.org/10.1590/S1517-707620200001.0883

[19] TENG, J.G., CHEN, S.T.S., LAM, L., *FRP-strengthened RC structures*, Chichester, John Wiley & Sons, 2002.

[20] BAKIS, C.E., BANK, L.C., BROWN, V.L., *et al*., "Fiber-reinforced polymer composites for construction—state-of-the-art review", *Journal of Composites for Construction*, v. 6, n. 2, pp. 73–87, 2002. doi: http://dx.doi.org/10.1061/(ASCE)1090-0268(2002)6:2(73)

[21] YIN, P., HUANG, L., YAN, L., *et al*., "Compressive behavior of concrete confined by CFRP and transverse spiral reinforcement. Part A: experimental study", *Materials and Structures*, v. 49, n. 3, pp. 1001–1011, 2016. doi: http://dx.doi.org/10.1617/s11527-015-0554-1

[22] YAN, L., CHOUW, N., KASAL, B., "Experimental study and numerical simulation on bond between FRP and CFRC components", *Journal of Reinforced Plastics and Composites*, v. 36, n. 4, pp. 305–320, 2017. doi: http://dx.doi.org/10.1177/0731684416683453

[23] ZHANG, S.S., KE, Y., CHEN, E., *et al*., "Effect of load distribution on the behaviour of RC beams strengthened in flexure with near-surface mounted (NSM) FRP", *Composite Structures*, v. 279, pp. 114782, 2022. doi: http://dx.doi.org/10.1016/j.compstruct.2021.114782

[24] SARIBIYIK, A., CAGLAR, N., "Flexural strengthening of RC Beams with low-strength concrete using GFRP and CFRP", *Structural Engineering and Mechanics*, v. 58, n. 5, pp. 825–845, 2016. doi: http://dx.doi.org/10.12989/sem.2016.58.5.825

[25] ASKAR, M.K., HASSAN, A.F., AL-KAMAKI, Y.S.S., "Flexural and shear strengthening of reinforced concrete beams using FRP composites: A state of the art", *Case Studies in Construction Materials.*, v. 17, pp. e01189, 2022. doi: http://dx.doi.org/10.1016/j.cscm.2022.e01189

[26] SHAKIR ABBOOD, I., ODAA, S., HASAN, K.F., *et al*., "Properties evaluation of fiber reinforced polymers and their constituent materials used in structures: a review", *Materials Today: Proceedings*, v. 43, pp. 1003–1008, 2021. doi: http://dx.doi.org/10.1016/j.matpr.2020.07.636

[27] LANDESMANN, A., SERUTI, C.A., BATISTA, E.M., "Mechanical properties of glass fiber reinforced polymers members for structural applications", *Materials Research*, v. 18, n. 6, pp. 1372–1383, 2015. doi: http://dx.doi.org/10.1590/1516-1439.044615

[28] BAGHERPOUR, S. Fibre reinforced polyester composites, In: H.E.D. Saleh (Ed.), *Polyester*, Croatia, InTech, pp. 135–166, 2012. doi: http://dx.doi.org/10.5772/48697

[29] GARCEZ, M., MENEGHETTI, L., SILVA FILHO, L.C., "Structural performance of RC beams poststrengthened with carbon, aramid, and glass FRP systems", *Journal of Composites for Construction*, v. 12, n. 5, pp. 522–530, 2008. doi: http://dx.doi.org/10.1061/(ASCE)1090-0268(2008)12:5(522)

[30] HOSNY, A., SHAHEEN, H., ABDELRAHMAN, A., *et al*., "Performance of reinforced concrete beams strengthened by hybrid FRP laminates", *Cement and Concrete Composites*, v. 28, n. 10, pp. 906–913, 2006. doi: http://dx.doi.org/10.1016/j.cemconcomp.2006.07.016

[31] XIONG, G.J., YANG, J.Z., JI, Z.B., "Behavior of reinforced concrete beams strengthened with externally bonded hybrid carbon fiber-glass fiber sheets", *Journal of Composites for Construction*, v. 8, n. 3, pp. 275–278, 2004. doi: http://dx.doi.org/10.1061/(ASCE)1090-0268(2004)8:3(275)

[32] HAWILEH, R.A., RASHEED, H.A., ABDALLA, J.A., *et al*., "Behavior of reinforced concrete beams strengthened with externally bonded hybrid fiber reinforced polymer systems", *Materials & Design*, v. 53, pp. 972–982, 2014. doi: http://dx.doi.org/10.1016/j.matdes.2013.07.087

[33] TAMIL SELVI, D., SAKTHIVEL, D.P.B., POORNIMA GANDHI, R., "Strengthening of reinforced concrete beam elements by wrapping with GFRP", *IJET*, v. 7, pp. 30, 2018. doi: http://dx.doi.org/10.14419/ijet.v7i3.34.18710

[34] Indian Standard, *IS 10262: Concrete mix design as per Bureau of Indian standards*, New Delhi, India, Bureau of Indian Standards, 2019.

[35] Indian Standard, *IS 456: Plain and Reinforced Concrete-Code of Practice*, New Delhi, India, Bureau of Indian Standards, 2000.

[36] American Society For Testing And Materials, *ASTM D3039: Test Method for Tensile Properties of Polymer Matrix Composite Materials*, West Conshohocken, PA, USA, ASTM International, 2008. doi: https://doi.org/10.1520/D3039_D3039M-08

[37] American Society For Testing And Materials, *ASTM D790: Test Methods for Flexural Properties of Unreinforced and Reinforced Plastics and Electrical Insulating Materials*, West Conshohocken, PA, USA, ASTM International, 2017. doi: https://doi.org/10.1520/D0790-17

[38] ACI Committee 440, *440.2R-17: Guide for the Design and Construction of Externally Bonded FRP Systems for Strengthening Concrete Structures*, Farmington Hills, American Concrete Institute, 2017. https://doi.org/10.14359/51700867

[39] CHOOBBOR, S.S., HAWILEH, R.A., ABU-OBEIDAH, A., *et al*., "Performance of hybrid carbon and basalt FRP sheets in strengthening concrete beams in flexure", *Composite Structures*, v. 227, pp. 111337, 2019. doi: http://dx.doi.org/10.1016/j.compstruct.2019.111337

[40] CHELLAPANDIAN, M., PRAKASH, S.S., SHARMA, A., "Experimental and finite element studies on the flexural behavior of reinforced concrete elements strengthened with hybrid FRP technique", *Composite Structures*, v. 208, pp. 466–478, 2019. doi: http://dx.doi.org/10.1016/j.compstruct.2018.10.028

[41] CHAWLA, K.K., *Composite Materials,* New York, Springer, 1998. doi: https://doi.org/10.1007/978-1-4757-2966-5

[42] ZHANG, C., LIANG, C., LIANG, T., *et al*., "Enhanced mechanical properties of an Mg-Zn-Ca alloy via high pressure torsion and annealing for use in bone implantation.", *Matéria (Rio de Janeiro)*, v. 27, n. 3, pp. 1–12, 2022. doi: http://dx.doi.org/10.1590/1517-7076-rmat-2022-0005

[43] CHAPETTI, M.D., "Fracture mechanics models for short crack growth estimation and fatigue strength assessment.", *Matéria (Rio de Janeiro)*, v. 27, n. 3, pp. 1–11, 2022. doi: http://dx.doi.org/10.1590/1517-7076-rmat-2022-0030

[44] FURIAN, B.O., PIMENTEL, L.L., FORTI, N., *et al*., "Mechanical behavior analysis of concrete with recycled aggregate and addition of steel and AR glass fiber.", *Matéria (Rio de Janeiro)*, v. 27, n. 1, pp. 1–20, 2022.